Single-Walled Carbon Nanotubes Mediated Neovascularity Targeted Antitumor Drug Delivery System

Chengqun Chen[a,*], Huijuan Zhang[a,*], Lin Hou[a], Jinjin Shi[a], Lei Wang[a], Chaofeng Zhang[a] Mingyue Zhang[a], Hongling Zhang[a], Xiufang Shi[a], Huixiang Li[b], Zhenzhong Zhang[a,*]

[a] School of Pharmaceutical Sciences, Zhengzhou University, Zhengzhou, China
[b] Department of Pathology, The First Affiliated Hospital, Zhengzhou University, Zhengzhou, China

Received, June 9, 2012; Revised, January 5, 2013; Accepted, January 16, 2013; Published, January 16, 2013.

ABSTRACT: Purpose. The aim of this study was to prepare a new neovascularity targeting antitumor drug delivery system mediated by single-walled carbon nanotubes (SWNTs). **Methods.** In this study, antiangiogenesis agent 2-methoxyestradiol was loaded by SWNTs via π~π accumulation. The SWNTs were then linked with NGR (Asn-Gly-Arg) peptide, which could target tumor angiogenesis. This drug delivery system was characterized by transmission electron microscope, scanning electron microscopy, and atomic force microscope analysis. The suppression efficacy of tumor growth in cultured breast cancer cell line was evaluated by the 3-(4,5-dimethylthiazol-2-yl)-2,5-diphenyltetrazolium bromide assay. The in vivo antitumor activity was evaluated on the Sarcoma (S180) tumor-bearing mice model. **Results.** The characteristics of this drug delivery system showed that the particle of complex was 190 ± 4.3 nm in size distribution and –23.56 ± 2.03 mV in zeta potential. The inhibition ratio of this SWNTs drug delivery system at 24, 48, and 72 h was about 57.7%, 83.6%, and 88.2%. Compared with normal saline group, the relative tumor volumes in the 2ME, SWNTs-2ME, and NGR-SWNTs-2ME groups were decreased 1 week after administration. **Conclusion.** This novel neovascularity targeting drug delivery system containing NGR-SWNTs-2ME may be beneficial to improve treatment efficacy and minimize side effects in future cancer therapy.

INTRODUCTION

New blood vessel formation is important for tumor growth, and antiangiogenesis is a novel approach for cancer therapy (1). Endothelial cells of the angiogenic vessels within solid tumors express several proteins that are absent or barely detectable in normal blood vessels, including integrin $\alpha_v\beta_3$ and $\alpha_v\beta_5$, aminopeptidase, vascular endothelial growth factor receptor, matrix metalloproteinase, proteoglaycan, and prostate-specific membrane antigen. Some of them are already used as targets for tumor-specific targeting delivery. Among the various new targeting ligands, peptides containing the sparagine–glycine–arginine (NGR) motif have been shown to home into tumors by binding with CD13 receptor (2).

Antiangiogenesis agent 2-methoxyestradiol (2ME) inhibits the growth of cancer cells (gastric, angiosarcoma, cervical, hepatocellular, colorectal, lung, prostate, breast, pancreatic, neuroblastoma, leukemia, multiple myeloma) (3-5). One of most interesting feature of 2ME is the inhibition of the pro-angiogenic transcription factor hypoxia-inducible factor 1-alpha, so it leads to reduced expression of some tumor angiogenesis growth factors (6). Targeted drug delivery to cancer cells or tumor tissues can enhance the therapeutic effect while reducing or preventing toxic side effects associated with chemotherapy (7). To targeted deliver the novel antiangiogenesis agent 2ME to the tumor site, we combined 2ME with NGR (new blood vessel formation targeting ligands) using single-walled carbon nanotubes (SWNTs) as a carrier. Under physiological tumor conditions, nanoparticles ranging from 100 to 200 nm in diameter have a significant chance of targeting to the leaky vessels of tumor tissue, termed the enhanced permeability and retention (EPR) effect (8). This therapy of 2ME combining with NGR targeting of tumor blood vessels could be a viable strategy for cancer therapy.

Within the family of nanomaterials, SWNTs have emerged as a new vehicle for the delivery of

Corresponding Author: Zhenzhong Zhang, School of Pharmaceutical Sciences, Zhengzhou University, Zhengzhou, China. Email: zhangzz08@126.com

therapeutic molecules into cells (9). With all atomies exposed on the surface, SWNTs have ultrahigh area that permits efficient loading of multiple molecules along the length of the nanotube sidewall (10). Supramolecular binding of aromatic molecules can be easily achieved by π-π stacking of those molecules onto the polyaromatic surface of nanotubes (11). SWNTs can effectively shuttle various biomolecules including drugs, peptides, proteins, plasmid DNA, and small interfering RNA into cells via endocytosis (12). In our previous study, docetaxel delivered by SWNTs show better tumor-suppressive effects than docetaxel alone (13). These characteristics make SWNTs a viable candidate carrier for 2ME and NGR.

For the NGR-SWNTs-2ME complex preparation, 2ME was attached through π-π accumulation to SWNTs and dispersed in water with poloxamer 188 (Pol-188), phosphatidylcholine (PC), and 1,2-distearoyl-sn-glycero-3-phosphoethanolamine -*N*-[methoxy (polyethylene glycol)-2000] (DSPE-PEG2000)-Maleimide (DPM). The maleimide group at the end of DPM on the surface of SWNTs can react with the double bond in the sulfhydryl groups. The maleimide reacted with cysteine in $CNGRCK_2HK_3HK_{11}$(C containing sulfhydryl groups) and connected covalently. The suppression efficacy of tumor growth of NGR-SWNTs-2ME complex was evaluated through cultured MCF-7 cell line by 3-(4,-dimethylthiazol-2-yl)-2,5-diphenyltetrazolium bromide (MTT) assay and S180 tumor-bearing mice model in vivo.

MATERIALS AND METHODS

SWNTs were purchased from Chengdu Organic Chemicals Co. Ltd, Chinese Academy of Sciences. 2ME (99.5% in purity) was home-made. PC (injection grade) was purchased from Zhengzhou Siwei Phospholipid Technology (Zhengzhou, China). Pol-188 was obtained from BASF Co. Ltd. NGR peptides ($CNGRCK_2HK_3HK_{11}$) were compounded by Shanghai Botai Biotechnology Co. Ltd. (Shanghai, China). DPM and other reagents were all purchased from Sigma. A MCF-7 human breast cancer cell line and S180 mouse ascites tumor cells were obtained from the Chinese Academy of Sciences Cell Bank. Experimental animals were provided by the Henan Laboratory Animal Center.

Preparation of NGR-SWNTs-2ME

Ten milligram of SWNTs was mixed with 40 mg 2ME in 2 mL of anhydrous ethanol using an ultrasonic bath for about 30 minutes while 5 mL of ultrapure water was added dropwise. The mixture was sonicated using an ultrasonic probe (400 W, 3 s × 15 times). The remaining solids were thoroughly rinsed with anhydrous ethanol to remove excess 2ME. The complex of SWNTs-2ME was collected for the next preparation.

The SWNTs-2ME was mixed in an aqueous solution of PC (1.2 mg/mL), Pol-188 (2.8 mg/mL), and DPM 0.1 mg/mL, and the solution was then sonicated using an ultrasonic probe (400 W, 3 s × 15 times). The solution was then filtered through a membrane filter (Whatman, Maidstone, UK) with a pore size of 100 nm to remove the excess surfactants, rinsed thoroughly with water, and then centrifuged at 4000 rpm for 15 minutes and repeated to remove macromolecular particles. The complex of DPM-SWNTs-2ME was prepared for the next NGR peptide conjugation.

NGR peptide water solution was added to the DPM-SWNTs-2ME suspension, which was modified by surfactant, and DPM with NGR and maleimide in a molar ratio of 1:15. After being left to stand overnight at room temperature, NGR-SWNTs-2ME was obtained. The solid was washed with water through a membrane filter to remove excess uncombined NGR. Thin-layer silica gel chromatography was used to monitor the reaction of NGR and SWNTs-2ME was accomplished.

Determination of drug loading efficiency of 2ME

NGR-SWNTs-2ME was diluted with dimethyl sulfoxide (DMSO) and sonicated to ensure that the 2ME was dissolved completely and then centrifuged to separate the SWNTs and 2ME to determine the amount of 2ME bound to the SWNTs. The concentration of 2ME in DMSO was determined by high-performance liquid chromatography (HPLC). The HPLC conditions were as follows: an Eclipse XDB-C18 column (4.6 mm × 150 mm, 5 μm) (Agilent USA); mobile phase consisting of methanol and water 70/30; flow rate 1.0 mL/min; column temperature 30°C; fluorescence detection wavelength E_x = 288 nm, E_m = 325 nm; injection volume: 20 μL. Absorbance at 808 nm (A_{808}) was used to determine the SWNTs concentration in the suspension by visible spectrophotometry.

Characterization of NGR-SWNTs-2ME

Determination of size distribution and zeta potential

NGR-SWNTs-2ME at a concentration of 10 μg/mL was determined to obtain mean size and zeta potential. The size distribution and zeta potential of the nanosuspension was determined at 25°C using a Nano ZS-90 (Malvern Instruments, UK).

Transmission electron microscopy

Three to five drops of NGR-SWNTs-2ME nanosuspension were placed onto a copper grid, and the excess liquid was removed by touching one edge of the grid with filter paper, then the copper grid with NGR-SWNTs-2ME was dried under infrared light and scanned by transmission electron microscope (TEM) (JEM-1200EX, JEOL, Japan).

Scanning electron microscope

A drop of NGR-SWNTs-2ME nanosuspension was placed onto a small piece of silicon stuck to a metal stub and evaporating residual water using a hot plate. Scanning electron microscope (SEM) images were acquired using FEI2000 Nova Nano SEM system.

Cytotoxicity

MCF-7 cells were seeded in 96-well plates and treated with different concentrations of NGR-SWNTs for 72 h to investigate the cytotoxicity of the delivery system alone and then of NGR-SWNTs-2ME, SWNTs-2ME, or 2ME for 24, 48, and 72 h, respectively. Cell viability was measured using MTT assay.

Animal model and In vivo therapeutic effect in a S180 tumor-bearing mice

All care and treatment of the animals used in this study was performed in accordance with the guidelines for the Care and Use of Laboratory Animals published by the National Institutes of Health. The S180 tumor model was generated by subcutaneous injection of 2×10^6 cells in 100 μL phosphate-buffered solution into the right shoulder of female BALB/c mice. The mice were treated when the tumor volume reached 100 mm^3 (7 days after tumor inoculation).

The mice were divided into five groups (n = 6 per group) to receive different treatments of normal saline (control group), NGR-SWNTs, NGR-SWNTs-2ME, SWNTs-2ME, or 2ME respectively. The injected doses were normalized to be 4 mg/kg. The study preparations were injected into the mice via the caudal tail vein every 2 days. The mice were observed daily, and the tumor size was measured by a vernier caliper every alternate day. The tumor volume was calculated as (tumor width)^2 × (tumor length)/2. The relative tumor volumes were calculated as V/V_0 (V_0 was the tumor initial volume).

Biodistribution of 2ME and targeting efficiency

The S180 tumor model mice of experimental groups and the control group were given NGR-SWNTs-2ME, SWNTs-2ME, or 2ME (2ME in each group at 8 mg/kg) via the caudal tail vein. At 0.25, 1, and 3 h after administration, the tissues/organs (heart, liver, spleen, lung, kidney, brain, and tumors) were collected, weighed, and homogenized in methyl for biodistribution analyses. 2ME concentrations in tissues were analyzed by HPLC/FLD.

The biodistribution of 2ME was investigated in tumors and in various organs in the mice for clarifying the tumor treatment efficacy of the different 2ME formulations (NGR-SWNTs-2ME, SWNTs-2ME, and 2ME). To quantitatively evaluate the targeting characteristics of NGR-SWNTs-2ME in vivo, several parameters were calculated, including targeting efficiency (TE), the percentage of drug distribution in the tissues. The formula applicable to all tissues is as follows:

$$TE = \frac{(AUC_{0-3h})i}{\sum_{i=1}^{n}(AUC_{0-3h})} \times 100\% \quad (1)$$

TE is the targeting efficiency and AUC_{0-3h} is the area under the curve, the calculation of AUC_{0-3h} was performed using a trapezoidal method.

Preparation of NGR-SWNTs-FITC and tissue distribution study using fluorescence microscopy

To evaluate the NGR-SWNTs targeting drug delivery system in vivo distribution, fluorescein isothiocyanate (FITC) was conjugated with NGR-SWNTs and SWNTs. 0.2 mL of FITC in dimethyl sulfoxide (1 mg/mL) was added to 10 mL of NGR-SWNTs or SWNTs and then the mixture was sonicated and protected from light. Gel chromatography was used to remove the excess FITC by loading 5 mL of the solution onto a Sephadex G-25 column (Sigma). When the elution solvent (ultrapure water) was flown

through the column, the formation of two separate bands was observed. The fractions were collected, and the absorbance of the various fractions was measured at 488 nm with a spectrophotometer. Fractions from the first elution peak were pooled because they were attributed to the higher molecular weight NGR-SWNTs-FITC conjugate (also confirmed by fluorescence measurement).

The S180 tumor-bearing mice were given NGR-SWNTs-FITC (SWNTs in each group at 7.2 mg/kg) via the caudal tail vein. The tissues/organs (heart, liver, spleen, lung, kidney, brain, and tumor) were collected 3 h after administration and immediately frozen in powdered dry ice for 30 minutes. The prepared specimens were embedded in tissue optimum cutting temperature-freeze medium and refrozen for cryostat sectioning (3–5 μm in thickness). All tissue samples were observed by fluorescence microscopy (Nikon 80I) and performed green light density statistics.

STATISTICAL ANALYSIS

Quantitative data were expressed as mean ± SD. Means were compared using Student's *t* test. *P* values of <0.05 were considered statistically significant. All analyses were performed with SPSS 15.0 statistical software.

RESULTS

Preparation of NGR-SWNTs-2ME

In this study, the dispersion effect of several surfactants on SWNTs was tested. Pol-188 and PC had a good dispersion effect for SWNTs, but the drug loading capabilities were different when their ratios changed at the same total concentration. The drug loading was highest (SWNTs to 2ME ratio about 1:0.956) at the concentration of 2.8 mg/mL and 1.2 mg/mL for Pol-188 and PC, respectively (Figure 1).

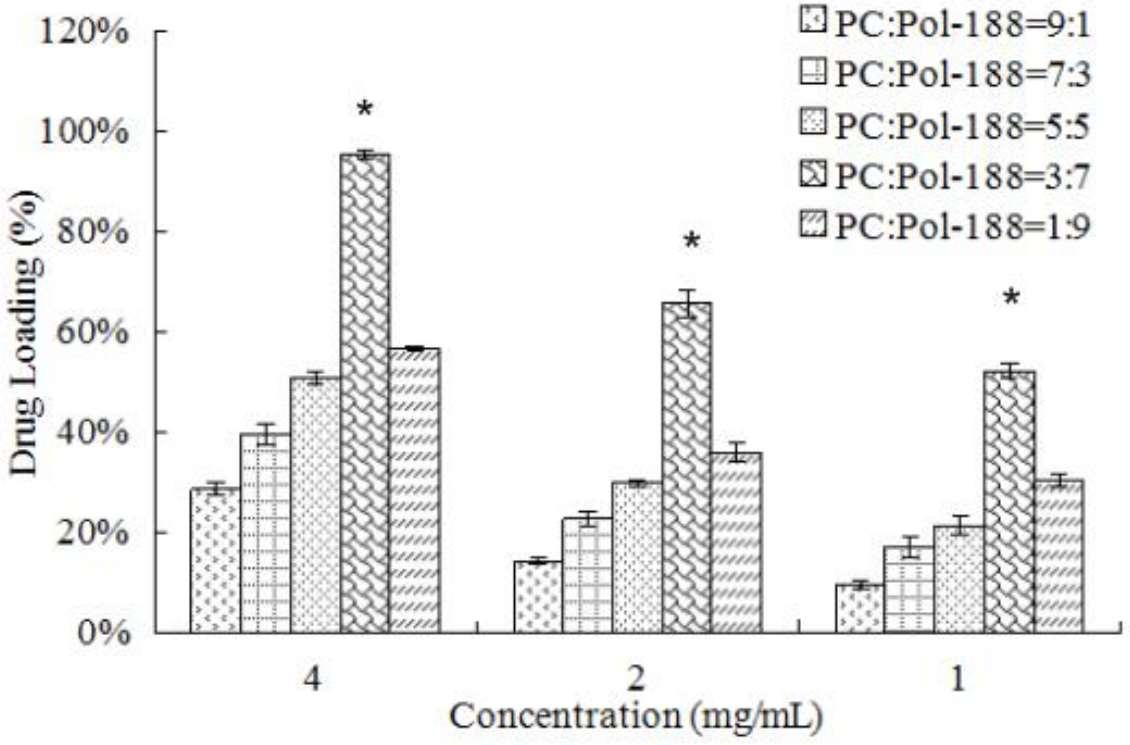

Figure 1. Effects of different ratios of PC and Pol-188 on drug loading. Concentrations of PC and Pol-188 were 4, 2, and 1 mg/mL. Data are presented as the mean ± standard deviation (n = 3). *P < 0.05, versus other ratio of PC and Pol-188 at 4 mg/mL.

Characterization of NGR-SWNTs-2ME

Size distribution is a very important parameter for nanomedicine and it affects performance in vivo. For the treatment of tumors and cancer, 100–200 nm nanoparticles are attractive because of the unique feature known as the EPR effect (8). As electric charges repel each other, zeta potentials on the surface of the nanoparticles can prevent them from flocculation and keep the system stable. Zeta potential of the NGR-SWNTs-2ME particle was –22.66 ± 3.03 mV (Figure 2A), and size distribution was 185 ± 4.0 nm (Figure 2B). It is noteworthy that NGR-SWNTs-2ME solution can keep stable for several weeks or even months without aggregation (Figure 2C). The TEM image of NGR-SWNTs-2ME demonstrated that drugs and surfactants attached around SWNTs (Figure 3A, 3B). The SEM image of NGR-SWNTs-2ME showed that the particle was unequally dimensioned isolated particles with a diameters of ~50 nm and length of ~200 nm (Figure 3C) , which was consistent with the result of size distribution.

Cytotoxicity

A toxicity assay was performed to examine the potential toxicity of NGR-SWNTs. When the concentration of NGR-SWNTs was lower than 22 μg/mL, the survival rate of the MCF-7 cells was more than 95% during 48 h. It revealed that the NGR-SWNTs had no significant cytotoxicity to the MCF-7 cells.

The proliferation of MCF-7 cells was inhibited by the 2ME, SWNTs-2ME, and NGR-SWNTs-2ME groups. The inhibition rates were positively correlated with dose and time. When the time period was 72 h and the dose was 10.15 μg/mL, the inhibition ratio of NGR-SWNTs-2ME was about 88.2%. The inhibition rates at different dose and different time (24, 48, and 72 h) were significantly different (Figure 4).

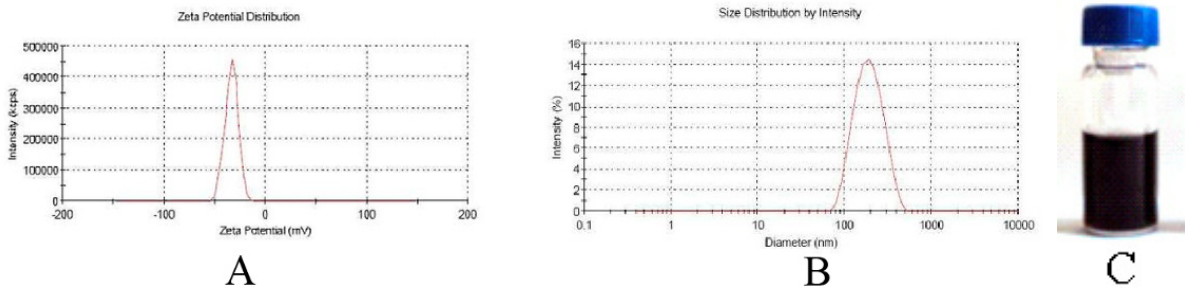

Figure 2. Characterization of NGR-SWNTs-2ME. (A) zeta potential; (B) size distribution; (C) solubility of NGR-SWNTs-2ME for 4 weeks.

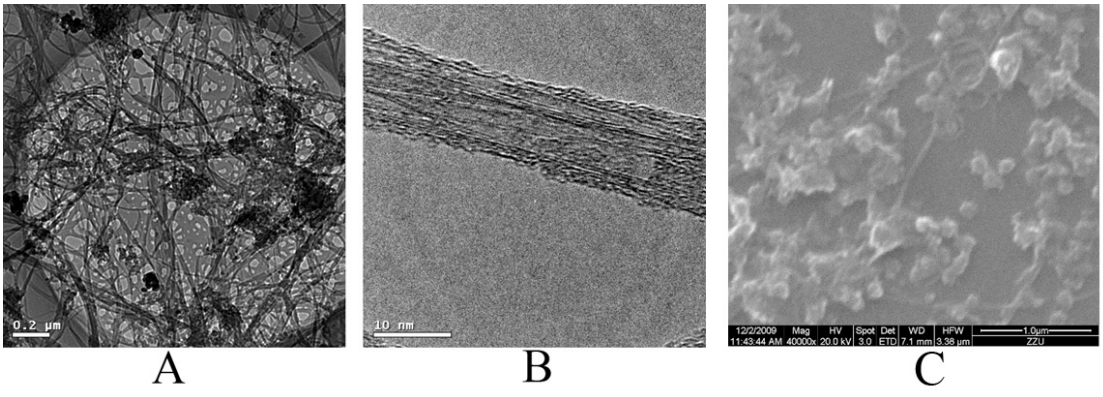

Figure 3. Characterization of NGR-SWNTs-2ME using TEM (A, B), and SEM (C, the scale bar was 1.0 μm; HV, 20.0 KV; WD, 7.7 mm; Mag, 40,000×).

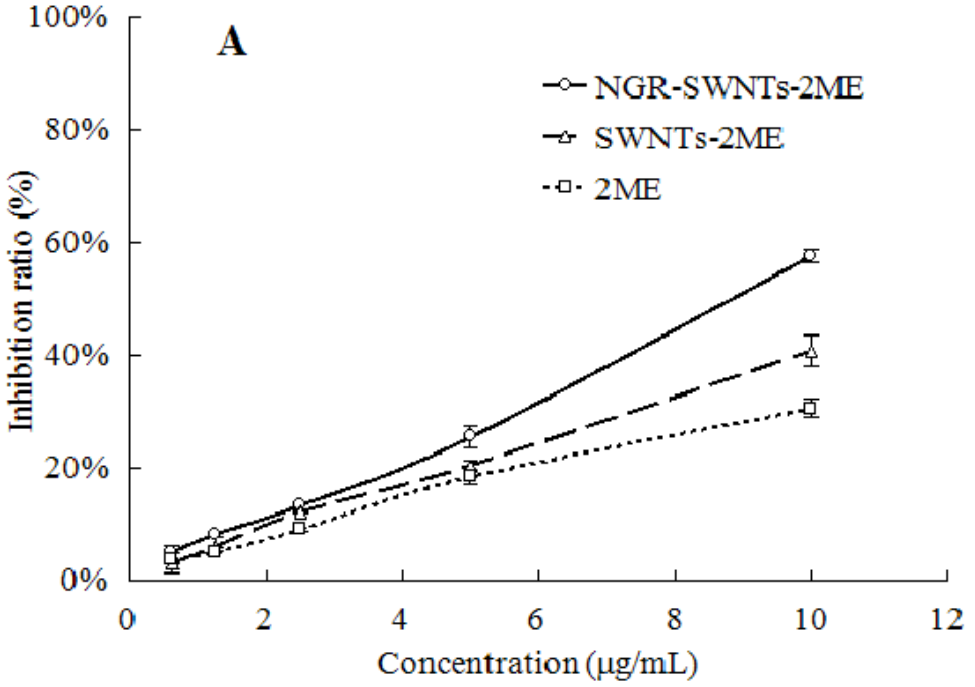
A
NGR-SWNTs-2ME
SWNTs-2ME
2ME
Inhibition ratio (%)
100%
80%
60%
40%
20%
0%
0
2
4
6
8
10
12
Concentration (μg/mL)

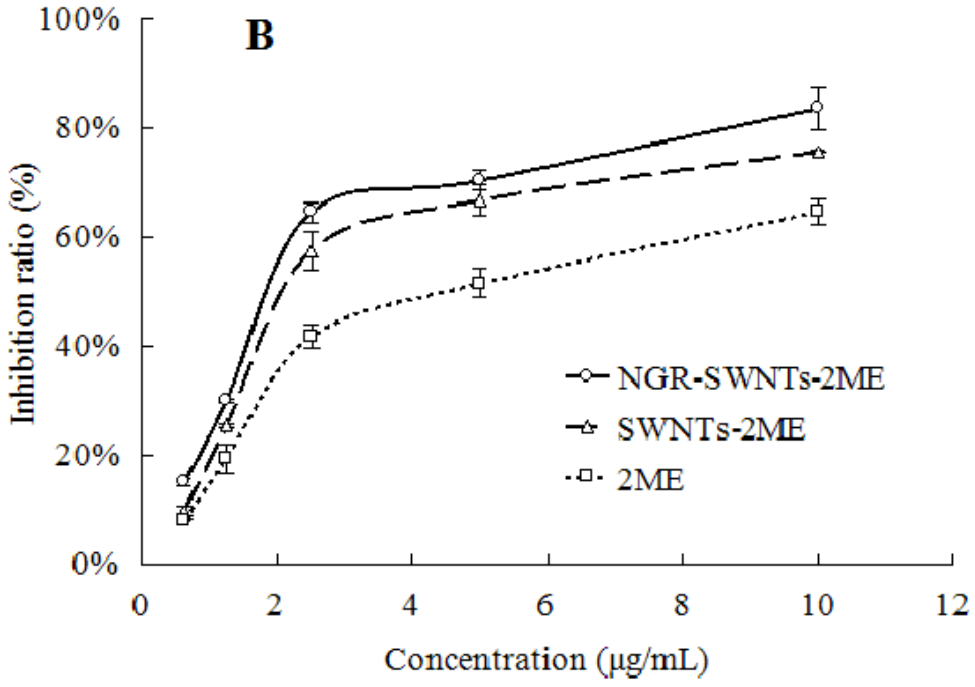
B
NGR-SWNTs-2ME
SWNTs-2ME
2ME
Inhibition ratio (%)
100%
80%
60%
40%
20%
0%
0
2
4
6
8
10
12
Concentration (μg/mL)

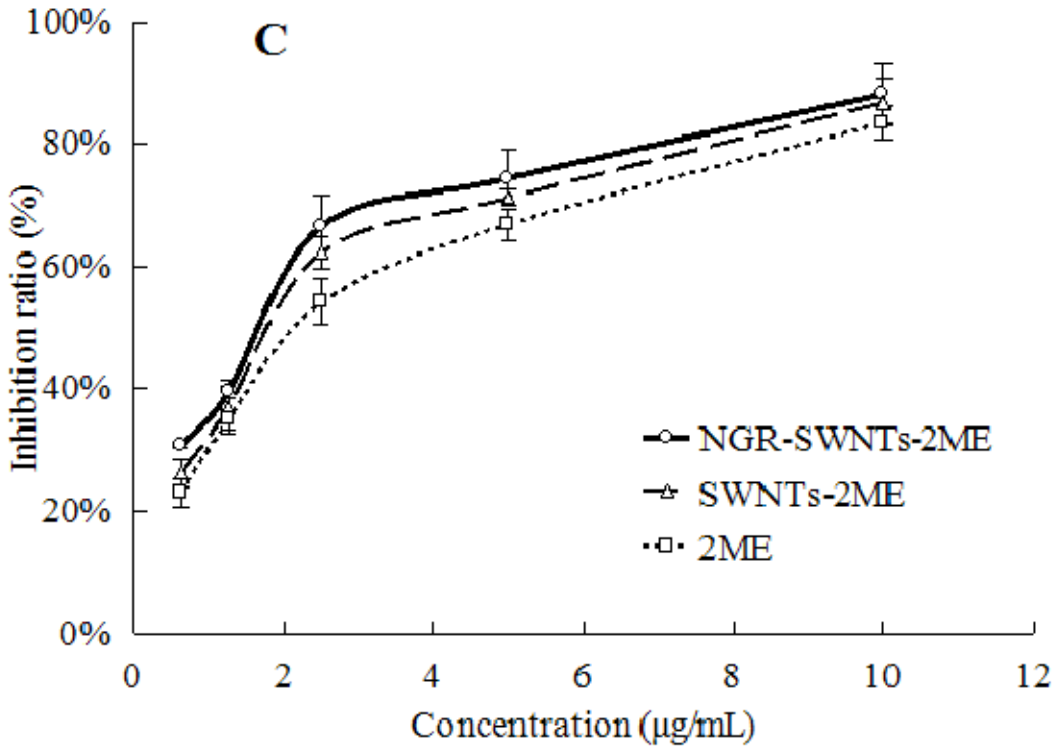

Figure 4. Inhibition ratios of 2ME, SWNTs-2ME, and NGR-SWNTS-2ME in MCF-7 cells. The inhibition ratios at 24 h (A) and 48 h (B) time points for the 2ME and NGR-SWNTs-2ME groups were significantly different ($P < 0.05$). However, at the point of 72 h (C), there was no significant difference between NGR-SWNTs-2ME, and SWNTs-2ME ($P > 0.05$), while there was significant difference between NGR-SWNTs-2ME and 2ME group ($P < 0.05$).

In vivo therapeutic effect on S180 tumor-bearing mice

Compared with normal saline group, the relative tumor volumes in the 2ME, SWNTs-2ME, and NGR-SWNTs-2ME groups were decreased 1 week after administration. Efficacy in the NGR-SWNTs-2ME group was superior to that in the SWNTs-2ME group and 2ME group and was markedly different from both the SWNTs-2ME group and the 2ME group (Figure 5).

Biodistribution of 2ME and targeting efficiency

The calculation of $AUC_{0\text{-}3h}$ of 2ME was performed for the biodistribution of 2ME administered in the different 2ME formulations (NGR-SWNTs-2ME, SWNTs-2ME, and 2ME) (Figure 6). Only little 2ME reached tumor tissue when the drug was administered alone. The $AUC_{0\text{-}3h}$ of 2ME in NGR-SWNTs-2ME for the tumor was markedly higher than the 2ME group, while for the lung it was significantly reduced. Compared with SWNTs-2ME group, distribution of 2ME of NGR-SWNTs-2ME group in heart, spleen, and kidney was decreased, while distribution in tumor tissues was significantly increased.

The targeting or distribution efficiency values for NGR-SWNTs-2ME in liver, lung, and tumor were changed compared with the 2ME group (Figure 7), indicating good targeting of NGR-SWNTs-2ME to the tumor tissues. It may be contributed to NGR peptide, which could enhance the 2ME target to tumor tissue.

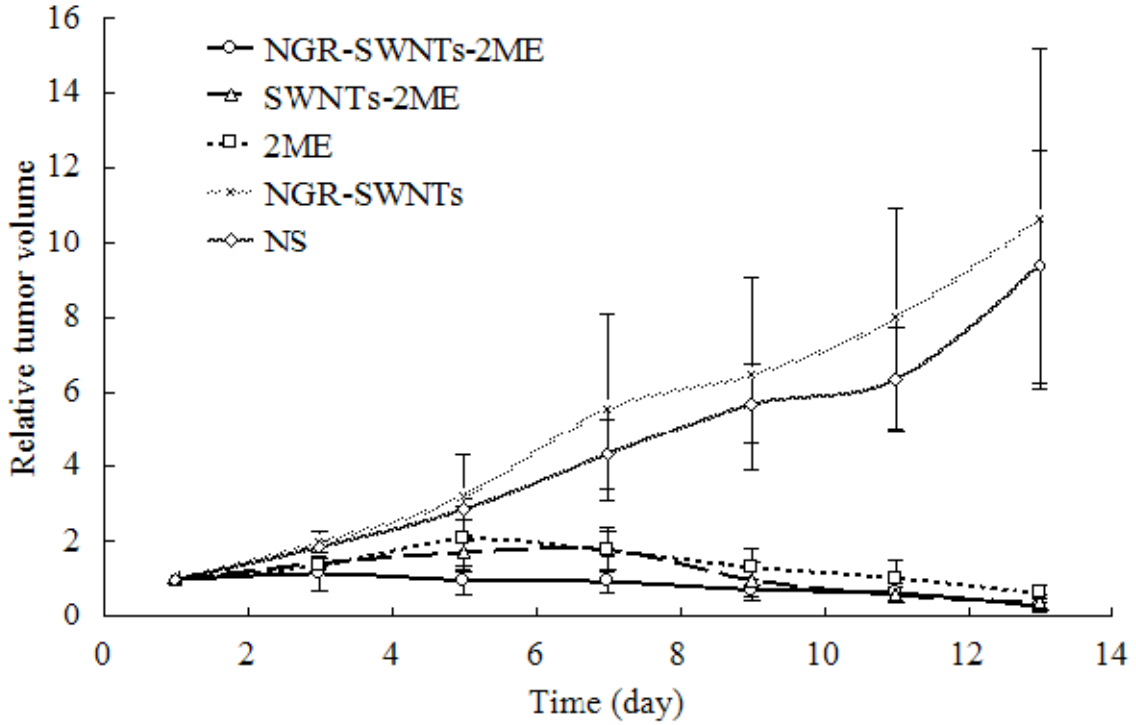

Figure 5. Average relative tumor volumes in S180 mice model of treatment in vivo. The SWNT-NGR-2ME-laser group shows significant ($P < 0.05$) suppression of tumor growth compared with the other experimental groups ($n = 6$).

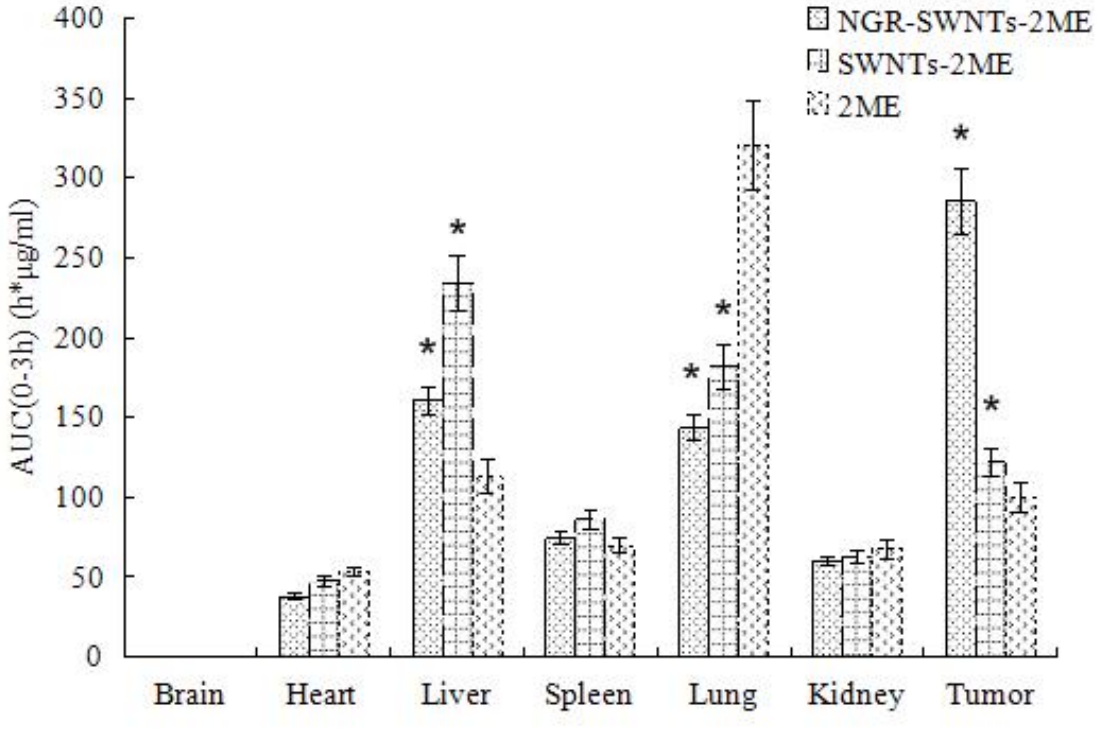

Figure 6. The $AUC_{0\text{-}3h}$ of 2ME in tissues of mice after administration of 2ME, SWNTs-2ME, and NGR-SWNTs-2ME. Data are presented as mean ± SD ($n = 6$). *$p < 0.05$, vs. 2ME group.

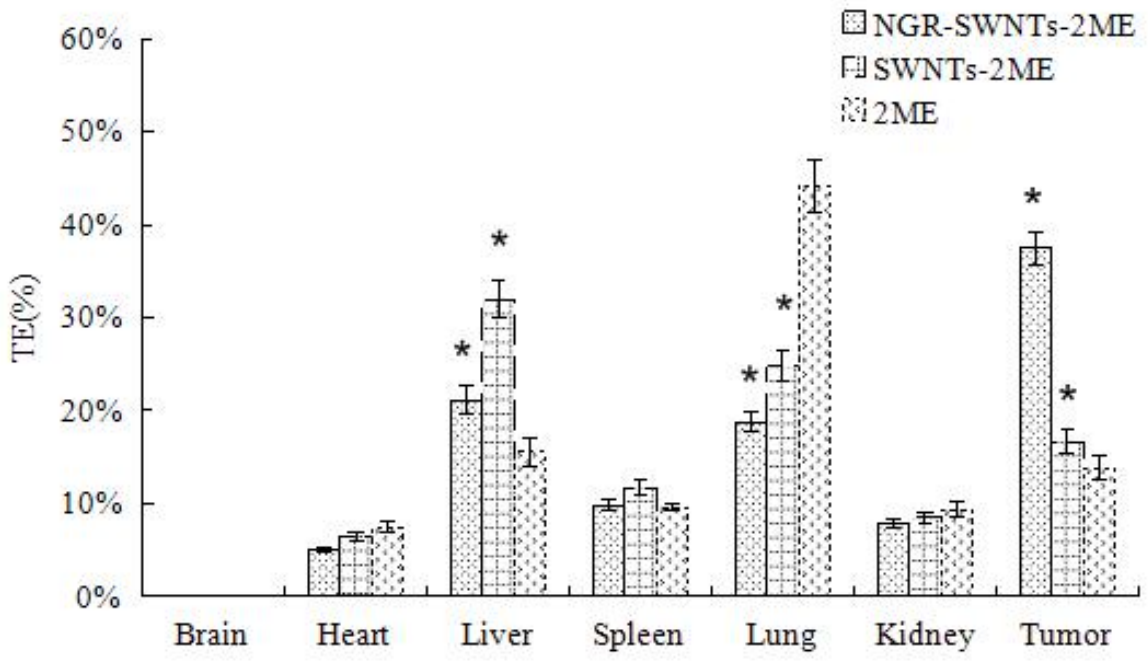

Figure 7. The targeting efficiency of 2ME in tissues of mice after administration of 2ME, SWNTs-2ME, and NGR-SWNTs-2ME. Data are presented as mean ± SD, (n = 6) *p < 0.05, vs. 2ME group.

Tissue distribution study using fluorescence microscopy

Fluorescence image of the tissues' (heart, liver, spleen, lung, kidney, brain, and tumor) frozen sections were observed at 3 h after injection of the NGR-SWNTs-FITC, SWNTs-FITC, or control group (FITC in NS solution) (Figure 8). Statistics of green light intensity was performed. Compared with other tissue, the fluorescent intensity in the tumor was significantly higher, suggesting that the NGR peptide may enhance the targeting ability of NGR-SWNTs delivery system to tumor tissue.

DISCUSSION

Morphology of blood vasculature in tumors and normal tissues is uniquely different: the unique vascular pathophysiology, microanatomy of tumors, and the biochemical mechanisms involved in the EPR effect. The size distribution of this NGR-SWNTs-2ME drug delivery system was about 180 nm, so it can be selectively delivered to the tumor tissue because of the EPR effect (8). The NGR peptide are targeted to the tumor new blood vasculature, and then this drug delivery system would retain in the tumor tissues, while the antitumor drug 2ME led to reduced expression of tumor angiogenesis growth factors. The blood vasculature of tumor can be blocked, and the tumor will be starved and suppressed. The significant tumor decrease after administration of NGR-SWNTs-2ME suggested that this neovascularity-targeted therapy strategy could be truly effective.

SWNTs have attracted tremendous attention because of their unique properties as one of most promising nanomaterials for a variety of biomedical application (14). SWNTs have the potential to be used in drug delivery system. Anticancer drugs (Gemcitabine, Daunorubicin, Paclitaxel, Platinum (IV), and Doxorubicin) have been reported to attach with SWNTs through either covalent or noncovalent bonding (15-19). All these drugs only directly inhibit tumor growth. In this study, we used a new antiangiogenesis agent 2ME and executed a new treatment strategy, which inhibited not only tumor cells but also the blood vasculature growth. The result of superior therapeutic efficacy of NGR-SWNTs-2ME in vitro and in vivo has proved this point.

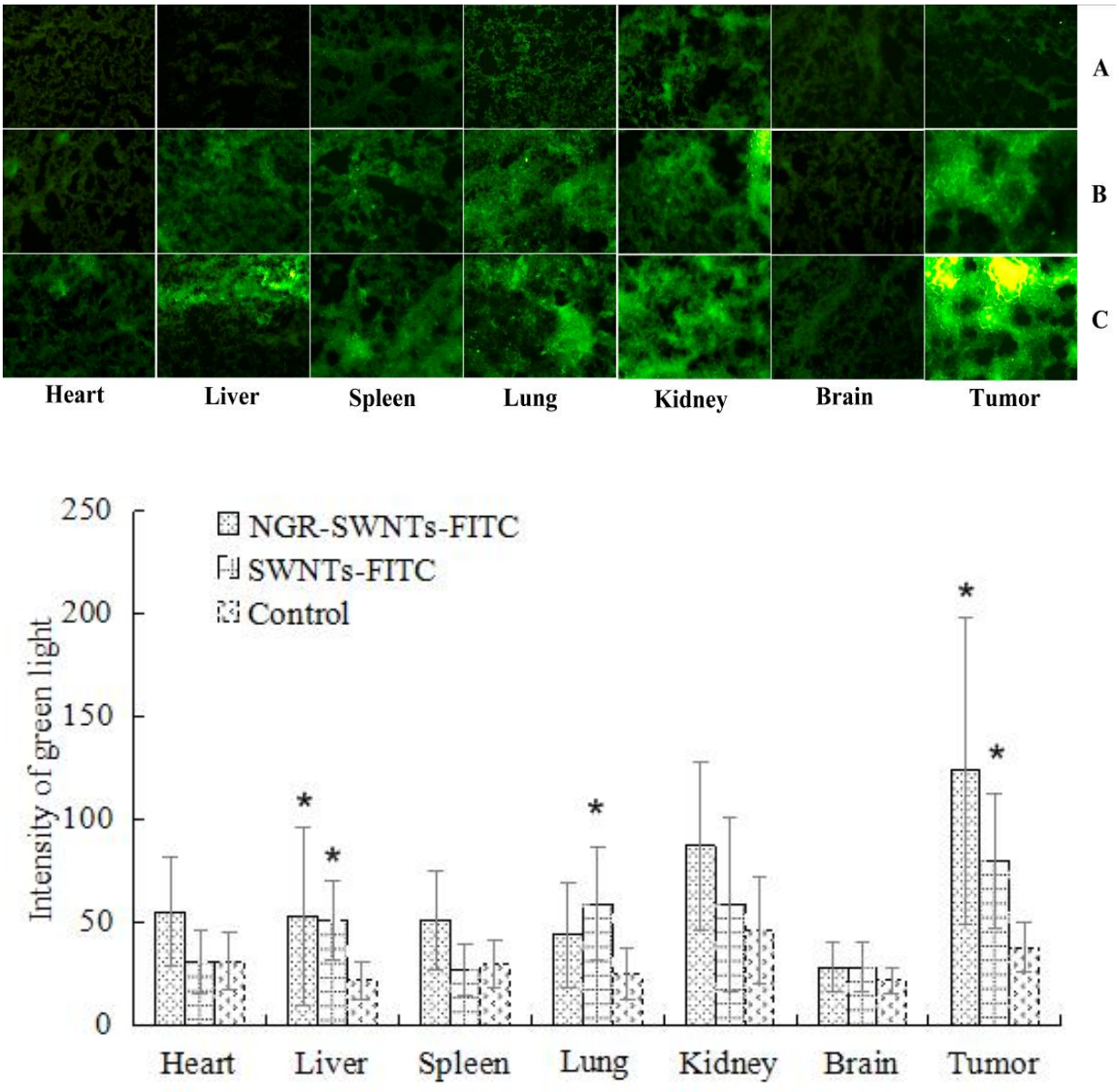

Figure 8. Fluorescence images and intensity of green light of tissues in S180 tumor-bearing mice. (A) Control; (B) SWNTs-FITC; (C) NGR-SWNTs-FITC; Data are presented as mean ± SD, (n = 6), *p < 0.05, vs. control group.

Fluorescence image of the tissues' frozen section suggested that NGR-SWNTs-FITC was detected mostly in tumor, secondly in liver, lung, and less in brain after injection. In an experiment carried out in the United States, mice were intratracheally instilled with a single dose of SWNTs; the biodistribution of SWNTs was the most in lung, secondly in liver and spleen, less in blood, which may be because the SWNTs were administrated intratracheally (14). 2ME distribution of NGR-SWNTs-2ME, SWNTs-2ME, and 2ME in tumor-bearing mice was shown as follows for the 2ME group, 2ME was detected mostly in lung, secondly in liver, and less in brain; for the SWNTs-2ME group, 2ME was detected most in liver, secondly in lung, and less in brain; for the NGR-SWNTs-2ME group, 2ME was detected mostly in tumor, secondly in liver and lung, and less in brain. This change of 2ME was related to the different carrier (SWNTs or NGR-SWNTs) of 2ME. As these results suggested, the SWNTs drug delivery system might be taken up by macrophages in liver and lung. These results are consistent with a previous study in

which SWNTs injected intravenously into rats were taken up by macrophages, primarily in the liver (20). The clearance route of SWNTs drug delivery system may point toward either biliary or renal pathways (21). Biocompatible nanoscale dispersion provides a scalable method to generate purified preparations of SWCNTs with minimal toxicity, thus allowing them to be used safely in biomedical applications (22).

There is another interesting feature of NGR-SWNTs targeting drug delivery system, which led to recent interest in the effect of near infrared light on SWNTs used for thermal treatment of cancer. In future study, administration of NGR-SWNTs-2ME to the tumor combined with thermal will be another good therapy strategy.

CONCLUSION

This neovascularity-targeting drug delivery system containing NGR-SWNTs-2ME reveals stronger tumor inhibition effect and targeting efficiency than 2ME alone and SWNTs-2ME without NGR. From these multifactor influences of tumor neovascularity, it may be promising for a new strategy in future cancer therapy.

ACKNOWLEDGEMENTS

This work was supported by grants from the National Natural Science Foundation of China (Nos. 30973660 and 30973482). Chengqun Chen and Huijuan Zhang contributied equally to this work.

REFERENCE

1. Sitohy B, Nagy JA, Dvorak HF. Anti-VEGF/VEGFR therapy for cancer: reassessing the target. Cancer Res. 2012; 72(8): 1909-1914.
2. Zhou T, Jia X, Li H, Wang J, Zhang H, A Y, et al. New tumor-targeted nanosized delivery carrier for oligonucleotides: characteristics in vitro and in vivo. Int J Nanomedicine. 2011; 6: 1527-1534.
3. Guo X, Xing Y, Mei Q, Zhang H, Zhang Z, Cui F. Preparation and cytotoxicity of 2-methoxyestradiol-loaded solid lipid nanoparticles. Anticancer Drugs. 2012; 23(2): 185-190.
4. Du B, Wang SY, Shi XF, Zhang CF, Zhang ZZ. The effect of 2-methoxyestradiol liposome on growth inhibition, angiogenesis and expression of VEGF and Ki67 in mice bearing H22 hepatocellular carcinoma. Tumori. 2011; 97(5): 660-665.
5. Du B, Zhao Z, Sun H, Ma S, Jin J, Zhang Z. Effects of 2-methoxyestradiol on proliferation, apoptosis and gene expression of cyclin B1 and c-Myc in esophageal carcinoma EC9706 cells. Cell Biochem Funct. 2012; 30(2): 158-165.
6. Zhang Q, Ma Y, Cheng YF, Li WJ, Zhang Z, Chen SY. Involvement of reactive oxygen species in 2-methoxyestradiol-induced apoptosis in human neuroblastoma cells. Cancer Lett. 2011; 313(2): 201-210.
7. Byrne JD, Betancourt T, Brannon-Peppas L. Active targeting schemes for nanoparticle systems in cancer therapeutics. Adv Drug Deliv Rev. 2008; 60(15): 1615-1626.
8. Maruyama K. Intracellular targeting delivery of liposomal drugs to solid tumors based on EPR effects. Adv Drug Deliv Rev. 2011; 63(3): 161-169.
9. Marches R, Mikoryak C, Wang RH, Pantano P, Draper RK, Vitetta ES. The importance of cellular internalization of antibody-targeted carbon nanotubes in the photothermal ablation of breast cancer cells. Nanotechnology. 2011; 22(9): 095101.
10. Gomez-Gualdron DA, McKenzie GD, Alvarado JF, Balbuena PB. Dynamic evolution of supported metal nanocatalyst/carbon structure during single-walled carbon nanotube growth. ACS Nano. 2012; 6(1): 720-735.
11. Wang C, Li S, Zhang R, Lin Z. Adsorption and properties of aromatic amino acids on single-walled carbon nanotubes. Nanoscale. 2012; 4(4):1146-1153.
12. Grigoryan G, Kim YH, Acharya R, Axelrod K, Jain RM, Willis L, et al. Computational design of virus-like protein assemblies on carbon nanotube surfaces. Science. 2011; 332(6033): 1071-1076.
13. Wang L, Zhang M, Zhang N, Shi J, Zhang H, Li M, et al. Synergistic enhancement of cancer therapy using a combination of docetaxel and photothermal ablation induced by single-walled carbon nanotubes. Int J Nanomedicine. 2011; 6: 2641-2652.
14. Madani SY, Naderi N, Dissanayake O, Tan A, Seifalian AM. A new era of cancer treatment: carbon nanotubes as drug delivery tools. Int J Nanomedicine. 2011; 6:2963-2979.
15. Kam NW, Dai H. Carbon nanotubes as intracellular protein transporters: generality and biological functionality. J Am Chem Soc. 2005; 127(16): 6021-6026.
16. Taghdisi SM, Lavaee P, Ramezani M, Abnous K. Reversible targeting and controlled release delivery of daunorubicin to cancer cells by

aptamer-wrapped carbon nanotubes. Eur J Pharm Biopharm. 2011; 77(2): 200-6.
17. Liu Z, Chen K, Davis C, Sherlock S, Cao Q, Chen X, et al. Drug delivery with carbon nanotubes for in vivo cancer treatment. Cancer Res. 2008; 68(16): 6652-60.
18. Dhar S, Liu Z, Thomale J, Dai H, Lippard SJ. Targeted single-wall carbon nanotube-mediated Pt(IV) prodrug delivery using folate as a homing device. J Am Chem Soc. 2008; 130(34): 11467-11476.
19. Liu Z, Fan AC, Rakhra K, Sherlock S, Goodwin A, Chen X, et al. Supramolecular stacking of doxorubicin on carbon nanotubes for in vivo cancer therapy. Angew Chem Int Ed Engl. 2009; 48(41):7668-7672.
20. Cherukuri P, Gannon CJ, Leeuw TK, Schmidt HK, Smalley RE, Curley SA, Weisman RB. Mammalian pharmacokinetics of carbon nanotubes using intrinsic near-infrared fluorescence. Proc Natl Acad Sci U S A. 2006; 103(50):18882-1886.
21. Bhirde AA, Patel S, Sousa AA, Patel V, Molinolo AA, Ji Y, Leapman RD, Gutkind JS, Rusling JF. Distribution and clearance of PEG-single-walled carbon nanotube cancer drug delivery vehicles in mice. Nanomedicine (Lond). 2010; 5(10):1535-1546.
22. Mutlu GM, Budinger GR, Green AA, Urich D, Soberanes S, Chiarella SE, Alheid GF, McCrimmon DR, Szleifer I, Hersam MC. Biocompatible nanoscale dispersion of single-walled carbon nanotubes minimizes in vivo pulmonary toxicity. Nano Lett. 2010; 10(5):1664-1670.